

# NF-κB Inhibition Activity of Curcumin-Loaded Sterically Stabilized Micelles and Its Up-Regulator Effect on Enhancement of Cytotoxicity of a New Nano-Pirarubicin Formulation in the Treatment of Breast Cancer

**Zahra Eskandari<sup>1,2</sup>, Fatemeh Bahadori<sup>1\*</sup>, Melda Altikatoglu Yapaoz<sup>1\*</sup>, Vildan Betul Yenigun<sup>3</sup>, Abdurrahim Kocyigit<sup>3</sup> and Hayat Onyuksel<sup>4</sup>**

<sup>1</sup>*Department of Chemistry, Biochemistry Division, Faculty of Sciences and Arts, Yildiz Technical University, Istanbul, Türkiye*

<sup>2</sup>*Department of Pharmaceutical Biotechnology, Faculty of Pharmacy, Bezmialem Vakif University, Istanbul, Türkiye*

<sup>3</sup>*Department of Medical Biochemistry, Faculty of Medicine, Bezmialem Vakif University, Istanbul, Türkiye*

<sup>4</sup>*Department of Biopharmaceutical Sciences, University of Illinois at Chicago, Chicago, IL 60612, USA*

(Received September 8, 2018; Revised October 17, 2018; Accepted October 18, 2018)

**Abstract:** This study aims to investigate the effects of co-administration of nano-Curcumin on anticancer effect of nano-Pirarubicin considering the fact that the clinical use of Pirarubicin and other anthracyclines has been limited by development of multidrug resistance (MDR) and based on previous data which have shown that Curcumin can down-regulate MDR proteins and suppress the activity of Nuclear factor-kappa B (NF-κB) a protein involved in chemoresistance. Nano micellar formulations of both Curcumin and Pirarubicin were separately synthesized using 1,2-Distearoyl-sn-glycero-3-phosphoethanolamine-N-methoxy-[poly(ethylene glycol); PEG MW 2,000] (DSPE-PEG2000). The produced sterically stabilized micelles (SSM) are very well known drug delivery systems in terms of their enhanced efficacy and good toxicity profile. We measured the differences of NF-κB levels in two different situations: when Pirarubicin is used alone and when it is co-administered with Curcumin. This study showed that co-administration of SSM-Curcumin (CSSM) and SSM-Pirarubicin (PSSM) with size of 12.81 nm enhances the efficacy of Pirarubicin by suppressing P65, an NF-κB subunit. Furthermore, we showed that SSM is able to successfully enhance water solubility and therapeutic stability of curcumin for using as a complementary agent.

**Keywords:** Curcumin; pirarubicin; nanoparticles; NF-κB; breast cancer. © 2019 ACG Publications. All rights reserved.

## 1. Introduction

During the recent years, the use of natural products during chemotherapy has become so common. Among these natural products, Curcumin is known as the most widely used. Curcumin is a hydrophobic polyphenol derived from the ancient Indian spice turmeric, the powdered rhizome of the herb *Curcuma longa* belonging to the ginger family [1]. Curcumin has a long history in Asian Indian medicine and has been used for the treatment of several disorders such as wound-healing, inflammation, cough, hepatic

\* Corresponding authors: E-Mail: [fatemehbahadori@gmail.com](mailto:fatemehbahadori@gmail.com) ; [maltikatoglu@yahoo.com](mailto:maltikatoglu@yahoo.com)

diseases, certain tumors and sinusitis [2]. The use of Curcumin in breast cancer chemotherapy seems to be a promising approach that can solve some of the issues in this field. Curcumin, has been the focus of an extensive amount of research in recent years due to its vast array of pharmacological activities including cancer chemopreventive and chemotherapeutic activities. Several studies have proved Curcumin to be an effective chemotherapeutic and chemopreventive agent [3, 4]. The anti-carcinogenic activity of Curcumin in breast cancer has been reported in several studies [5-7]. Several research studies have unveiled that Curcumin can also down-regulate multidrug resistance (MDR) proteins and P-glycoprotein in cancer cells [8] and thus it has the potential to defend the development of MDR in cancer cells. It is believed that development of resistance to Curcumin is very less likely as it induces cellular apoptosis via multiple cells signaling pathways. Curcumin can show pleiotropic effect due to its ability to inhibit multiple cell signaling pathways.

It has been revealed by intense research that Curcumin can inhibit cell proliferation, invasion, metastasis and angiogenesis by suppressing multiple cell signaling pathways. The transcription factor Nuclear factor-kappa B (NF-κB), constitutively expressed in almost all cancer types suppresses apoptosis in a wide variety of tumors [9]. NF-κB is the chief controller of inflammation, cell proliferation, apoptosis, and resistance in cells. Curcumin has the potential to suppress the activity of NF-κB [10] resulting in a subsequent down-regulation of many NF-κB regulated genes which are involved in tumorogenesis (e.g. TNF, COX-2, cyclin D1, c-myc and interleukins etc.). Curcumin demonstrated antitumor activity by inhibiting constitutive NF-κB activation and inducing apoptosis in tumor cells [11, 12]. Elevated NF-κB binding activity has been observed in both primary human breast cancer tissues and breast cancer cell lines, and contributes to the activation of CYCLIN D1, c-MYC, and MUC1 [9, 13-16].

However, despite the effectiveness of Curcumin against numerous human disorders, there are some issues that have been shown to limit its therapeutic efficacy in the clinic [17]. One of these issues is poor bioavailability of Curcumin. Multiple studies has shown that, even with high doses of Curcumin, the levels of Curcumin as well as its *in vivo* metabolites are extremely low in serum and tissues after a short period of time [18]. However, because of the multiple therapeutic potentials attributed to Curcumin, there has been a persistent search for a solution to these problems. The use of adjuvants that can block the metabolic pathway of Curcumin is the most common strategy for enhancing its bioavailability [19]. In addition, Nano-sized drug delivery systems are being sought as a way to overcome these limitations. Nanoparticle-based drug delivery systems have considerable potential for treatment of cancers and they are known as promising alternatives to traditional ways of treating cancer. The important technological advantages of nanoparticles used as drug carriers are high stability, high carrier capacity, feasibility of incorporation of both hydrophilic and hydrophobic substances, and feasibility of variable routes of administration. Drug delivery systems are considered to be efficient ways to minimize the side effects of anticancer drugs.

Some of the advantages of drug delivery systems were mentioned above. However, in our approach, we avoided to use usual carrying vehicles like DMSO due to its oxidation effects that can lead to misleading results. In addition, instead of commercial forms of Pirarubicin and Curcumin, the drug delivery system that is selected to be used here as a carrier is a micellar system named SSM (sterically stabilized micelles), made of 1,2-Distearoyl-*sn*-glycero-3-phosphoethanolamine-*N*-methoxy-[poly(ethylene glycol); PEG *MW* 2,000] (DSPE-PEG<sub>2000</sub>) and known to be totally nontoxic [20]. Using a carrier with a good toxicity profile paves the way for precise viability examinations as well as a better understanding of mechanisms involved.

One of the known chemicals used for cancer chemotherapy is Pirarubicin. Pirarubicin (4'-O-tetrahydropyranyl doxorubicin, THP), a tetrahydropyranyl-derivative doxorubicin, was found and developed by Umezawa *et al.* in 1979 [21]. Pirarubicin showed equal or superior cytotoxicity in cultured tumor cells, and less cardiotoxicity in hamsters compared to doxorubicin (DOX) [22, 23]. Pirarubicin is incorporated into cells about 170-times rapider than DOX in cultured tumor cells [9, 14, 22, 24]. Pirarubicin is clinically approved for head and neck cancer, stomach cancer, upper urinary tract cancer, uterus cancer, ovarian cancer, acute leukemia and malignant lymphoma in Japan. Unfortunately, the clinical use of Pirarubicin and other anthracyclines has been limited by their severe cardiotoxicity and the development of multiple drug resistance (MDR). In general, many patients achieve a complete

remission when initially treated with anthracyclines; however, ~70% of the patients eventually experience a relapse of the disease, and the treatment failure is mainly due to MDR.

Water solubility is another problem in using Pirarubicin. Even though there is no recorded exact value in literature for aqueous solubility of pirarubicin, it is well accepted that it is water insoluble [25] and our experience with the molecule also confirmed this fact. We have observed that Pirarubicin is soluble in methanol and not stably soluble in 5% DMSO in water. So administrating it using a nano carrier can reduce the needed dose and MDR as well as side effects.

Considering the facts mentioned above, this study aims to investigate the effects of co-administration of nano-Curcumin on anticancer effect of nano-Pirarubicin, a potent family of chemotherapeutic agents but known to develop MDR.

According to the feedback we have received from oncologists, in some cases, Curcumin is used two hours before chemotherapy while in some other cases it is used after chemotherapy. To find out which approach leads to a better result, we used Curcumin and Pirarubicin in different time intervals: before, after and at the same time, to show if there is any difference in the effect of Curcumin on viability of cancer cells in these three conditions.

In addition, considering the fact that inhibition of NF- $\kappa$ B is one of the most important effects of Curcumin, we measured the differences of NF- $\kappa$ B levels in two different situations: when Pirarubicin is used alone and when it is mixed with Curcumin. The main aim of this study was to study the possibility of inhibiting MDR by suppressing NF- $\kappa$ B using curcumin. Thus the cell lines resistant to chemotherapy was not used but development of MDR was studied by following the NF- $\kappa$ B sub-unit levels.

Furthermore, to find out NF- $\kappa$ B inhibitor effect of Curcumin arises from enol or keto tautomer, we used NMR spectrum of Curcumin in DMSO. Accepting the fact that the hydrophobic Curcumin will be incorporated with the hydrophobic core of SSM, DMSO, a solvent which is accepted as hydrophobic in high concentrations [26], is used in this assay. Figure 1 shows enol-keto tautomers and their equilibrium in Curcumin structure.

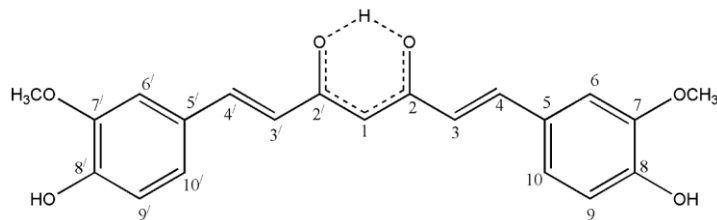


**Figure 1.** Tautomers of curcumin

## 2. Materials and Methods

### 2.1. Materials

1,2-Distearoyl-*sn*-glycero-3-phosphoethanolamine-*N*-methoxy-[poly(ethylene glycol); PEG  $M_W$  2,000] (DSPE-PEG<sub>2000</sub>) was obtained from santa cruz biotechnology (Texas, USA). Pirarubicin, Curcumin (>95.5%, #78246), Methanol, DMSO, Sulforudamin b, Acetic acid, Trichloroacetic acid, Dulbecco's modified Eagle medium (DMEM), penicillin-streptomycin and Trizma base were purchased from Sigma-Aldrich (Seelze, Germany), Trypsin-EDTA and Phosphate Buffered Saline from Gibco-Invitrogen, USA and fetal bovine serum (FBS) from Invitrogen Carlsbad, CA. MCF-7 human breast cancer cell line was obtained from ATCC (ATCC® HTB22™). Nuclear Extract and TransAM NF- $\kappa$ B Family Kits (40410 and 43296) from Active Motif, Carlsbad, CA.

### 2.2 Nuclear Magnetic Resonance (NMR) Studies on Curcumin

The structure analysis of Curcumin using NMR has previously been done by many groups [27, 28]. However, it is important to understand the tautomeric form of Curcumin inside of the hydrophobic core of SSM consisted of DSPE, which is accepted as the entrapment area of Curcumin. It is obvious that

this structure would be the source of the activity of Curcumin in all following experiments. NMR spectra were recorded on Varian Mercury-VX 400 MHz (400MHz for <sup>1</sup>H and 100 MHz for <sup>13</sup>C), in d-DMSO. Previously it has been shown that DMSO, in high concentrations behaves as a hydrophobic solvent [26]. Thus, *d*-DMSO has been used as a model for the hydrophobic environment of the core of SSM to identify Curcumin's structure there.

### *2.3. Preparation of Curcumin and Pirarubicin-loaded Sterically Stabilized Phospholipid Nanomicelles*

Curcumin-loaded sterically stabilized micelles (C-SSM) and Pirarubicin-loaded sterically stabilized micelles (P-SSM) formulations were prepared using a modified film rehydration/reconstitution technique. Briefly, solutions of 1 mM of DSPE-PEG<sub>2000</sub> in methanol with 200 µg/mL of Curcumin [29] and 100 µg/mL of Pirarubicin (our unpublished data) were prepared. The solutions were added to round bottom flasks and a thin film was obtained by remove of solvent using a vacuum rotary evaporator (Heidolph, Schwabach, Germany) under vacuum (125 mmHg pressure) at 45 °C and 150 rpm for 30 min. The films were kept in dark under vacuum overnight to make sure of elimination of residual solvent.

Then, the dried films were rehydrated with 1X PBS (pH 7.4), and the resulting dispersions were vortexed and sonicated for 5 min. Flasks were then sealed and allowed to equilibrate in dark for 2h at 25°C to produce C-SSM and P-SSM.

### *2.4. Characterization of Curcumin-loaded Nanomicelles*

#### *2.4.1. Particle size (PS) Measurement*

Nanoparticles mean diameter, PS distribution were determined by laser scattering light using Zetasizer Nano ZSP (Malvern Instruments Ltd, Malvern, UK) using a disposable cuvette. All measurements were carried out 3 times at 25°C. Default setting on the Zetasizer Nano ZS was used, i.e. refractive index, absorption, the dispersant used was water and measurement angle was 173. Measurements were repeated 5 times, 3 minutes each and data were analyzed by number distributions[30].

#### *2.4.2. Zeta Potential (ZP) Measurement*

The zeta potentials were measured using a Zetasizer Nano ZSP (Malvern Instruments Ltd, Malvern, UK). ZP was determined by laser Doppler micro-electrophoresis method by using a folded capillary zeta cell (Malvern Instruments Ltd). All measurements were carried out 3 times at 25°C.

#### *2.4.3. Lyophilization Studies*

Nanoparticles were lyophilized by FreeZone 2.5 plus LABCONCO Lyophilizer. 1 mL of different formulations were freezed at -80 °C overnight before placing in Lyophilizer for overnight drying under vacuum [31]. The maintained cakes were rehydrated with distillated water and equilibrated at 25°C for 2h before particle size analysis.

#### *2.4.4. Differential Scanning Calorimetry (DSC)*

The study of association of drugs with SSM should be done in aqueous system [31] while system is in its native micellar form. However, the ingredients' peaks will cover the peaks of drugs and drug delivery system since ratio of their amount will be far higher than drug and carrier. Since freeze-drying doesn't make any changes in the structure and composition of drug SSM formulations [32], lyophilization was used to eliminate the effect of water. DSC thermograms were recorded by controlled heating 5°/min using DSC 250 TA.

#### 2.4.5. Cytotoxicity of C-SSM and P-SSM Against MCF-7 Cells

MCF-7 Cells were cultured in DMEM media supplemented with 10% FBS and 100 U/mL penicillin–streptomycin at 5% CO<sub>2</sub> at 37°C. At 85% confluence, cells were harvested and subcultured according to experimental requirements.

Cytotoxicity of C-SSM and P-SSM was evaluated on MCF-7 human breast cancer cells by sulforhodamine B assay. Briefly, 12,000 cells/well were seeded in 96-well plates and were allowed to attach overnight. Cells were treated with five half-diluted solution series of C-SSM and constant concentrations of P-SSM. Administration of formulations were done in three different approaches: simultaneous, prior and posterior. “Free” Curcumin and Pirarubicin were dissolved in 0.5 % DMSO at the same concentrations of the formulations as positive controls. Empty SSM at lipid concentration corresponding to the highest lipid concentration of formulations, as well as DMSO and PBS (pH 7.4), were used as vehicle controls. Plates were incubated for 72h at 37°C in 5% CO<sub>2</sub>-humidified atmosphere. Thereafter, cell viability was determined by the sulforhodamine B cytotoxicity assay as previously described [20]. Optical density (OD) of acetic acid-fixed sulforhodamine B-stained cells was measured at 515 nm using a VARIOSKAN FLASH, Thermo scientific ELISA Reader. OD values from the treated samples were normalized to that of PBS-treated control. The half maximal inhibitory concentrations (IC<sub>50</sub>) were calculated using nonlinear regression analysis based on generated curves of survival percentage versus concentration.

#### 2.5. NF-κB Inhibition Activity

##### 2.5.1. Preparation of Cell Culture Lysates

MCF-7 cells were exposed to simultaneous administration of C-SSM and P-SSM formulations in 100 mm tissue culture dishes. Since there was no difference in the efficacy of P-SSM upon co-administration with, before or after C-SSM, they were applied together, while, 54μL of 200 μM Curcumin in SSM with 12 μL of 100 μM pirarubicin in SSM was applied on MCF-7 cells for 24 h. This was the optimized amount to obtain desired number of living cells for measuring the proteins at the end of the assay. After 24 h incubation at 37 °C cells were collected and the Nuclear and cytosolic extracts were obtained according to the Nuclear Extract Kit’s protocol (Active Motif North America). Bovine serum albumin was used according to Bradford assay’s protocol to measure the obtained extracts.

##### 2.5.2. Determination of NF-κB Amount

The amount of NF-κB family elements was measured in the extracts of treated and control MCF-7 cells using TransAm NF-κB Family kit (Active Motif, Inc.; cat. no.101046) according to the related protocol.

### 3. Results and Discussion

The aim in this study was, first, to determine the effect of different concentrations of nano-Curcumin on antitumor effects of nano-Pirarubicin in different administration intervals against human breast cancer and, second, to determine the effect of nano-Curcumin on NF-κB activity on MCF-7 breast cancer cells *in vitro*.

#### 3.1. 1D and 2D-NMR Spectra Results of Curcumin

These assays were conducted to understand the isomeric structure of Curcumin inside of the hydrophobic environment of nano drug delivery system. Previously, it has been shown that DMSO in high concentrations could be accepted as hydrophobic environment [26].

The <sup>1</sup>H NMR spectra of Curcumin shows a completely symmetric behavior by corresponding each peak to two symmetric protons, e.g. H-3 and H-3' are appeared together. (Supportive Data 1-4). The

conjugation of two keto groups at the middle of structure (carbon 2 and 2') causes observation of keto-enol tautomerism. Although it has previously been reported that the enol tautomer is the most stable isomer of Curcumin [33], it is still possible to detect two different peaks corresponded to each couple of protons, the short of which, is corresponded to the position of related proton in case of having the  $\beta$ -diketo tautomer in the structure (Supporting Data 1-4). Interestingly, the enol tautomer does not affect the symmetrical structure of Curcumin because of resonance (Figure 1). The most significant effect of keto-enol tautomerism is observed on the protons of the vinyl chain which are reported in Supporting Data 1. The transpositions of vinyl groups are confirmed by observing  $J = 16$  Hz between H-3 and H-4 and similarly between H-3' and H-4' (S3,4). It is well known that the protons near to keto groups are shielded by the pi system of C=O group [34]. This is the reason H-3 and H-3' are shifted to the upfield when the structure is in  $\beta$ -diketo position, while H-4 and H-4' show downfield shift. Similarly in  $^{13}\text{C}$ -NMR and APT spectra the  $\beta$ -diketo isomer specially effects the chemical shift of C-2,3 and 4 (S1 and S5-8). It is noteworthy that H-1 is appeared as one proton and detecting related peak corresponded to 2 protons is not possible due to circulation of the proton between the atoms attended is conjugation (S1-4).

Correlations between protons and carbons with direct bonds are confirmed using HSQC data (S9-11) and the neighboring protons are determined using COSY correlations which are reported in Supporting Data 1. Interestingly, due to the high number of conjugated systems, protons of three neighboring carbons show COSY correlations as well. COSY interactions between H-4 and H-9 and 10 is an example (S10-11). Three-bond HMBC correlations are observed e.g. between H-5 and C-9 (and between H-5' and C-5') (Figure 2, S-1 and S-14-15).

Finally, we could conclude that in hydrophobic environment (which is symbolized by DMSO in the NMR studies), the major structure of Curcumin is its enol tautomer, while  $\beta$ -diketo tautomer is still presented in the system as well. Our results are in well accordance with previously reported data [35].

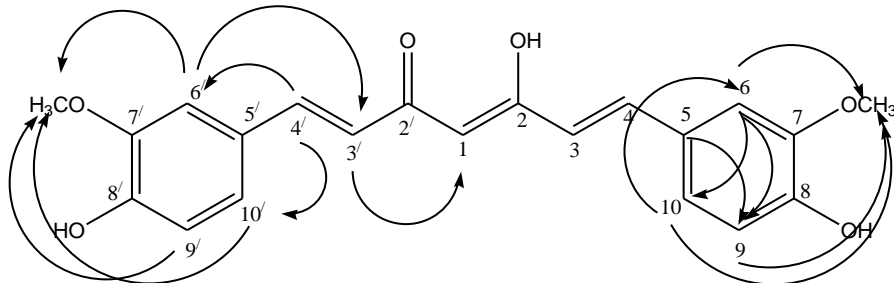


**Figure 2.** Selected HMBC correlations of the enol tautomer of curcumin

### 3.2. Characterization of C-SSM and P-SSM

The size of prepared C-SSM formulation was measured using Nano ZSP. C-SSM formulation showed hydrodynamic diameters of 12.81 nm (Figure 3-B), while, free SSM showed a diameter of 10.85 nm. These results are in well accordance with previously reported data (Figure 3-A) [36, 37].

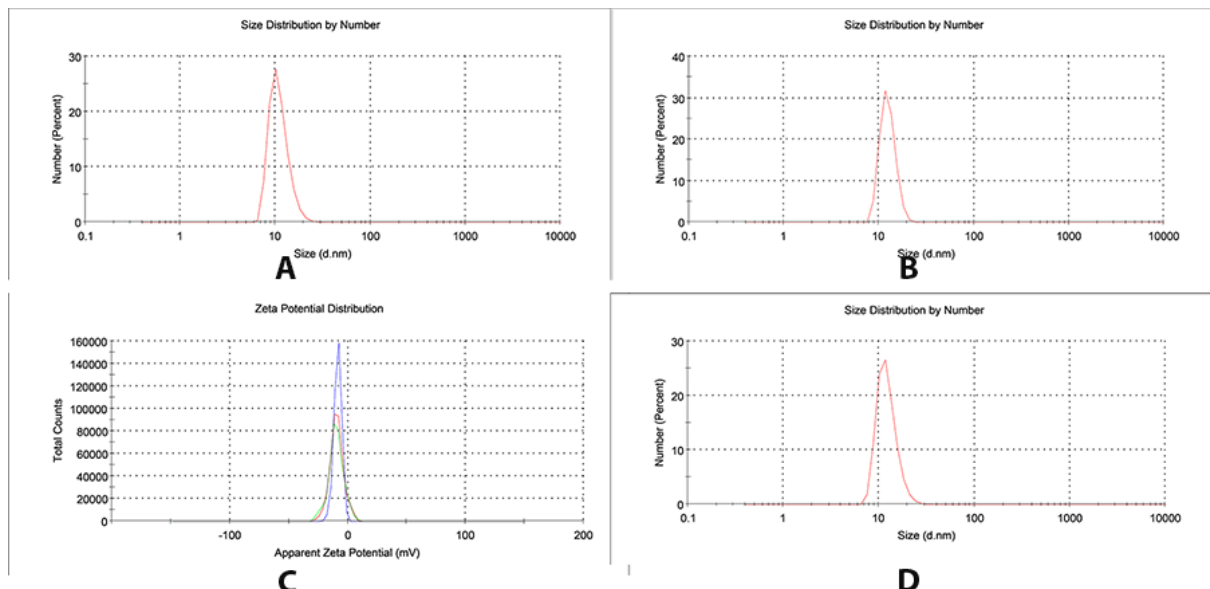


**Figure 3.** Zeta potential and size measurements result of C-SSM formulation obtained by DLS, A: Size distribution of free SSM =10.85, B: Size distribution of C-SSM as 12.81, C: Zeta potential of C-SSM equal to -8.43 and D: Size distribution of C-SSM after lyophilization and re-hydration

Particle size plays a major role in the mode of action of drug including the interaction of particles with a biological system, tissue distribution, attachment, and rolling [38]. Firm adhesion of nanoparticles, phagocytosis, and accumulation are all affected by the size of the particle [39]. Tailoring of a particle in a precise dimension ultimately leads to an incrimination in bio-distribution and longer circulation *in vivo*. The rate of excretion from the body is also high for large particles ( $> 1\mu\text{m}$ ). Larger particles get aggregated under physiological conditions and do not get filtered from capillaries [40].

The zeta potential of C-SSM formulation was found to be -8.43. Figure 3-C shows the zeta potential of C-SSM formulations.

The zeta potential indicates the degree of repulsion between adjacent, similarly charged particles in dispersion. “For particles that are small enough, a high zeta potential will confer stability, i.e., the solution or dispersion will resist aggregation” [41]. When nanoparticles are going to be introduced as a pharmaceutical agent, the surface charge of the nanoparticle is an important property that affects its circulation time. “The negatively charged particles reduce adsorption rate of serum proteins, resulting in longer circulation half-lives as compared to the positively charged particles” [42]. Positively charged particles have been reported to have a high non-specific rate of cellular uptake in most cells.

The stability of formulation after lyophilization was studied by the measurement of the size of nanoparticles. In the case of introduction of a formulation as a drug for clinic purposes, lyophilization and rehydration just before the usage is one of the best approaches. So, stability of formulation after rehydration is very important. As Figure 6 shows, the C-SSM showed a particle with a very similar size as one observed before lyophilization.

Differential scanning calorimetry (DSC) is a thermodynamic technique suitable for studying phase transitions. DSC studies were performed to evaluate the physical state of Curcumin and Pirarubicin in C-SSM, P-SSM nanoparticles. Figure 3-D shows the DSC thermograms of lyophilized micelles of Curcumin and Pirarubicin.

Previously, our group have reported the DSC thermogram of free SSM before and after micelle preparations [31]. As it has been shown, the thermogram of the hydrophobic part of SSM consisted of DSPE is observed at 48°C and that of the hydrophilic PEG is obtained at 52°C. These values are changed as 52°C and 54°C, respectively, after micelle preparation (S16-C). However, following uploading Curcumin to SSM both thermograms of DSPE and PEG shift to lower temperatures (S16-B). This not only shows the complete incorporation of the drug with the drug delivery system but also indicates the amorphous structure of both of them after loading process. It is obvious that the crystalline structure would cause obtaining related thermograms in higher temperatures (S16-B). Thus, we could hypothesize

that Pirarubicin is incorporating with both hydrophilic and hydrophobic parts of SSM. In contrast, uploading Curcumin to SSM causes complete separation of the thermograms of DSPE and PEG (S16-A), in which the significant increase in the intensity of the DSPE thermogram at 44.95°C shows the very firm interaction between Pirarubicin and SSM. The thermogram of PEG in P-SSM is almost similar to that in free SSM.

### 3.3 Investigation of *in vitro* Efficiency of C-SSM and P-SSM

The *in vitro* anticancer efficiency of free Curcumin and C-SSM formulation alone and mixed with P-SSM in three different application times were investigated on MCF-7 breast cancer cells. Cytotoxic effect of free Curcumin and C-SSM was found to be dose-dependent (Figure 4A and 4B). Free SSM was used as a control in its maximum concentration however it did not show toxicity on MCF-7 cells (data not shown).

As mentioned before, the concentration of P-SSM was kept constant (2 μL of 100μg/mL) and the related cytotoxicity percentages were 51.87%, 34.01% and 28.19% at 24h, 48h and 72h. C-SSM (9 μL of 200μg/mL) was administrated in successive double diluted solutions.

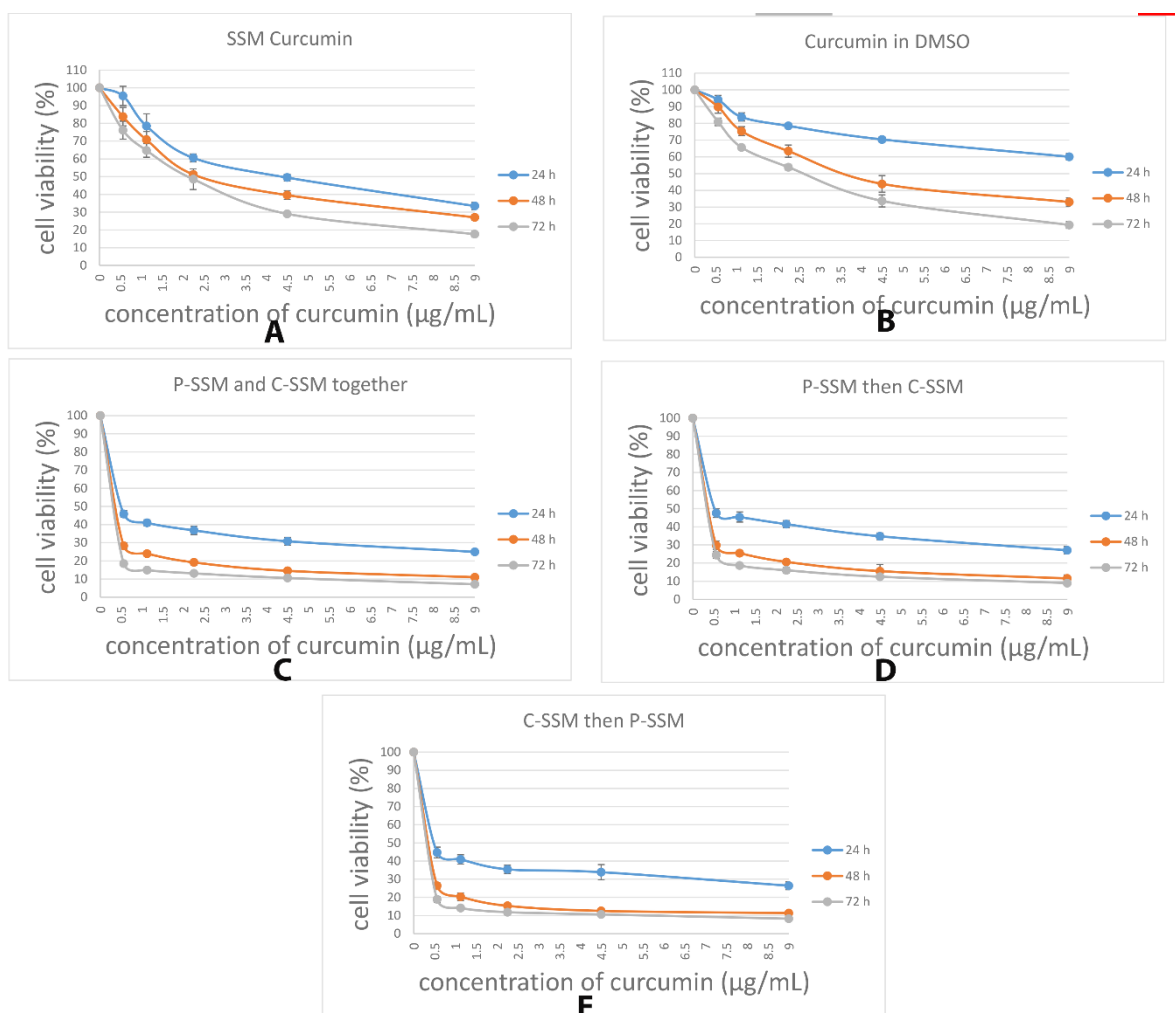


**Figure 4.** Cytotoxic effect of A: SSM-Curcumin in DMSO, B: Curcumin in DMSO, C: Co-administration of C-SSM and P-SSM, D: P-SSM while C-SSM was administered after one hour and E: C-SSM while P-SSM was administered after one hour (One-way ANOVA statistical analysis results are available at S18). Cell viability was calculated against control (Viability 100%).

Results of 72 h incubation of C-SSM and P-SSM are given in Figure 4C-E. Although the incubation resulted in significant reduction in cells viability, the results of one-way ANOVA revealed that the

viability in various administrations was not significantly different. The IC<sub>50</sub> values obtained from cytotoxicity assay are summarized in Table 1.

**Table 1.** The IC<sub>50</sub> values ( $\mu\text{g/mL}$ ) of application of Curcumin, C-SSM and co-administration of C-SSM and P-SSM in different orders

	24 h		48h		72 h	
	IC <sub>50</sub>	$\pm$	IC <sub>50</sub>	$\pm$	IC <sub>50</sub>	$\pm$
Curcumin in DMSO	11.158	0.511	5.264	0.493	3.591	0.248
C-SSM	5.557	0.180	4.220	0.082	3.065	0.098
SP and SC together						
SP then SC			All data were under 50% viability			
SC then SP						

### 3.4. NF- $\kappa$ B Inhibition Activity

Supplementary Data 17 represents the calibration curve of BSA that was used as a standard in determining the amount of extracted proteins.

Table 2 shows the measured amount of extracted proteins from control and treated MCF-7 cells. To measure NF- $\kappa$ B factors, the amount of these extracted proteins was normalized and applied to the NF- $\kappa$ B kit.

**Table 2.** The amount of extracted proteins (mg) from Control and treated MCF-7 cells

	Nuclear		Cytosolic	
	Extracted protein (mg)	$\pm$	Extracted protein (mg)	$\pm$
Control	0.676	0.0086	0.322	0.0073
C-SSM	0.588	0.0148	0.347	0.0108
P-SSM	0.738	0.0092	0.254	0.0203
Mix	0.630	0.017	0.304	0.0158

The MCF-7 cell line was used to examine the potential effects of C-SSM on NF- $\kappa$ B family members' amount in co-administration with P-SSM. This was approved in the present study as presented in Figure 5. This is the preliminary report on changes at P50, C-Rel and P52 activities upon treating MCF-7 cell lines with Pirarubicin and Curcumin. Generally P65 is reported as the reduced factor in inhibition studies of NF- $\kappa$ B [43-45].

The inactive form of NF- $\kappa$ B is localized in the cytoplasm and consists of three subunits: DNA-binding p50 and p65 subunits and I $\kappa$ B which is an inhibitory subunit and bound to p65. I $\kappa$ B masks the nuclear localization sequence. When it is released, the free NF- $\kappa$ B dimer then translocates to the nucleus where it recognizes and binds to specific DNA sequences [46]. NF- $\kappa$ B is constitutively expressed in almost all cancer types [47]. Moreover, it has been known that NF- $\kappa$ B is the chief controller of inflammation, cell proliferation, apoptosis, and resistance in cells. Curcumin has the potential to suppress the activity of NF- $\kappa$ B [48]. When we examined the P65 subunit in nuclear and cytosolic extractions of breast cancer cells, we observed that NF- $\kappa$ B is activated through the translocation of P65 from cytoplasm to nucleus. When (54 $\mu\text{L}$  of 200  $\mu\text{M}$ ) curcumin is applied with (12  $\mu\text{L}$  of 100  $\mu\text{M}$ ) pirarubicin to MCF-7 cells for 24 hrs, it was shown that amount of P65 decreased in the nuclear fractions in contrast to increasing amount in cytosolic fractions. This data shows that curcumin inhibits the translocation of P65 from cytoplasm to nucleus therefore inactivates NF- $\kappa$ B. Furthermore, as it could be seen in Figure 5, P65 amount was increased in nucleus when the cancer cells were treated with Pirarubicin. These results suggest that the use of Pirarubicin activates the NF- $\kappa$ B pathway and might be eventual cause of MDR. The amounts of each NF- $\kappa$ B subunit are given in Table 3.

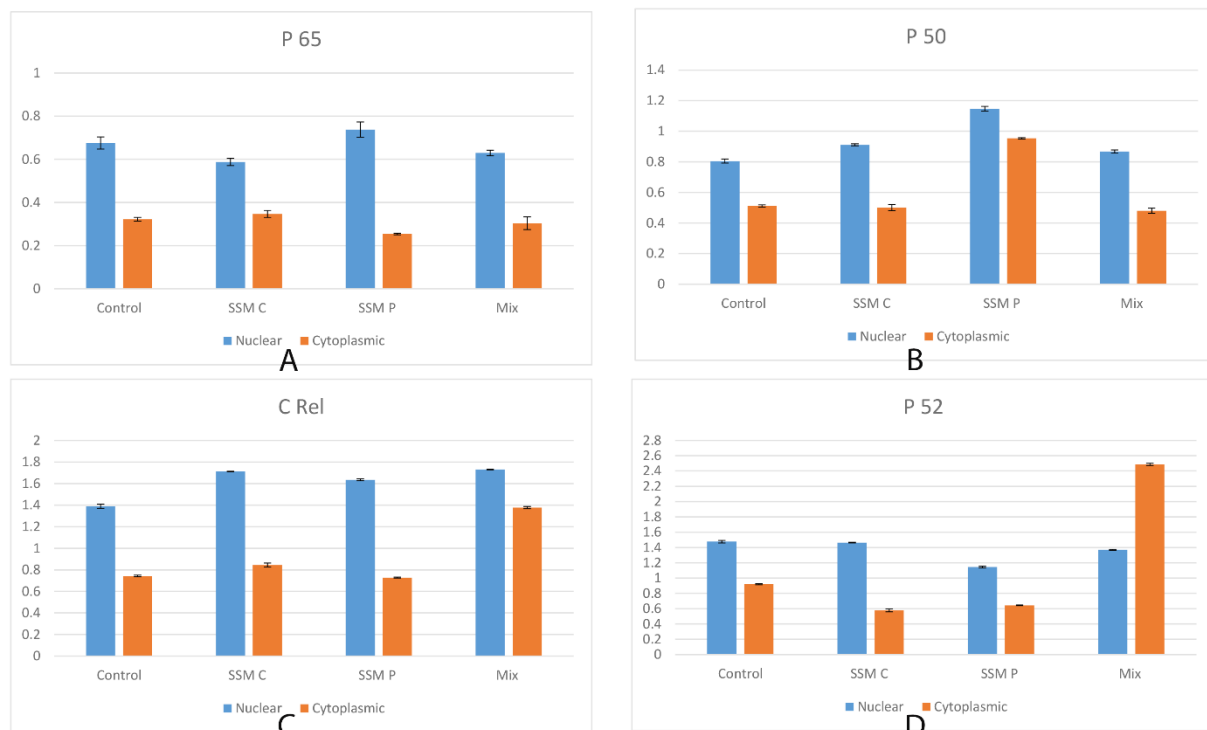


**Figure 5.** NF-κB family profiling of C-SSM, P-SSM treated and control MCF-7 cell. 54 μL of 200 μM Curcumin in SSM with 12 μL of 100 μM pirarubicin in SSM was applied on MCF-7 cells for 24 h. This was the optimized amount to obtain desired number of living cells for measuring the proteins at the end of the assay, A: P65, B: P50, CC Rel and D: P52

**Table 3.** Amounts of NF-κB subunits (μg/mL) after treating MCF-7 cells with C-SSM, P-SSM and their mixture

	Control		C-SSM		P-SSM		Mix		
	Amount	±	Amount	±	Amount	±	Amount	±	
P65	Nuclear	0.6757	0.0283	0.5877	0.0166	0.73779	0.0352	0.629571	0.02311
	Cytoplasmic	0.3223	0.0089	0.3471	0.0162	0.253869	0.0036	0.3035865	0.01563
P50	Nuclear	0.8052	0.0132	0.9116	0.0066	1.147	0.0156	0.8669	0.0635
	Cytoplasmic	0.5114	0.0071	0.5009	0.02	0.9538	0.0044	0.4802	0.0053
C Rel	Nuclear	1.3893	0.0193	1.7108	0.0028	1.6346	0.0079	1.7304	0.0065
	Cytoplasmic	0.743	0.0079	0.8449	0.0183	0.7281	0.0047	1.3776	0.0063
P52	Nuclear	1.4759	0.0162	1.4646	0.0047	1.1456	0.0117	1.3694	0.007
	Cytoplasmic	0.9206	0.0075	0.5778	0.0192	0.6442	0.0045	2.4875	0.0137

There are several limitations concerning systemic administration of single-drug chemotherapy, including fast blood/renal clearance, poor bioavailability and MDR. As mentioned before, it has been shown that the clinical use of anthracyclines was limited by the development of MDR. Even though, most of the patients achieve a complete remission when initially treated with this drug, ~70% of the patients eventually experience a relapse of the disease, and the treatment failure is mainly due to MDR. Different proteins including NF-κB transcription factors have been reported to contribute to chemoresistance [44, 49, 50].

Besides, drug accumulation at the tumor sites is often too low to reach an effective dose, requiring high drug dose during administration which in turn causes severe adverse side effects [51]. Moreover, single drug chemotherapies may not be potent enough to suppress all cancer cell growth given the inhomogeneous distribution of cancer cells within the tumors [52]. Recently, combination chemotherapy of multiple anticancer drugs has been extensively developed since it could reduce MDR and side effects

as a result of lower dosage of each drug [53]. It also includes co-administration of some natural products that are known as Integrative Medicine.

The MDR mechanisms of anthracyclines are complicated and not fully understood. Different proteins, genes and pathways have been reported to contribute to chemoresistance [54] among them NF- $\kappa$ B transcription factors are known to promote oncogenesis, increasing proliferation, survival, invasion, and metastasis by promoting transcription of proliferative, proinvasive, and anti-apoptotic genes [55, 56]. The NF- $\kappa$ B family, which consists of p65 (RelA), RelB, p50/105 (NF- $\kappa$ B1), c-Rel, and p52/p100 (NF- $\kappa$ B2), are constitutively activated in many cancers [56]. NF- $\kappa$ B is activated via the canonical pathway by Inhibitor of kB kinase (IKK $\beta$ )-dependent phosphorylation and degradation of I $\kappa$ B (which normally binds and inhibits p50/p65 dimers from entering the nucleus) [56]. NF- $\kappa$ B dimers translocate into the nucleus where they bind NF- $\kappa$ B response elements and promote transcription [57]. NF- $\kappa$ B post-translational modifications (e.g. phosphorylation and acetylation) regulate its nuclear localization, DNA binding, oligomerization, interaction with coactivators/ corepressors, and transactivation [56]. NF- $\kappa$ B promotes survival by inducing expression of anti-apoptotic proteins.

Daunorubicin, another member of anthracyclines family, has been shown to activate NF- $\kappa$ B and inhibition of NF- $\kappa$ B has been reported to lead to dramatically improved cell death response as compared to the parental cell line HT1080 [54, 58]. This phenomenon was observed in this work as well; an increase in the P65 level was observed in the cells that were treated with P-SSM in comparison with control. As was expected, administration of Pirarubicin led to an increase in P65.

Collectively, studies suggest the critical role that NF- $\kappa$ B plays in patients treated with various chemotherapeutic agents, emphasizing again that selective inhibition of NF- $\kappa$ B is critical. Therefore, finding a way to decrease MDR effect and to downregulate NF- $\kappa$ B pathway can be a significant step in diminishing the trappings of Pirarubicin application in treating breast cancer. Curcumin has a great potential to solve this issue.

Curcumin can inhibit cell proliferation, invasion, metastasis and angiogenesis by suppressing multiple cell signaling pathways. Curcumin shows antitumor activity by inhibiting constitutive NF- $\kappa$ B activation and inducing apoptosis in tumor cells [8]. Accordingly it has been [59] shown that Curcumin (20  $\mu$ M) significantly ( $p < 0.05$ ) suppressed NF- $\kappa$ B activation which was induced by gemcitabine (100 $\mu$ M) in both MCF-7 and MDA MB-231 cell lines. The combined results revealed the beneficial role of Curcumin in potentiating the anti-tumor effects of gemcitabine through NF- $\kappa$ B suppression and apoptotic effects.

It has been reported that [8] Curcumin contributes to the reversal of resistance to adriamycin in L1210/Adr cells. These effects were considered to result from the suppression of P-gp expression through inhibition of the PI3K/Akt/ NF- $\kappa$ B signaling cascade by Curcumin.

Curcumin has down-regulated NF- $\kappa$ B and growth control molecules induced by NF- $\kappa$ B in human pancreatic cells [60]. These effects were accompanied by marked growth inhibition and apoptosis. The results presented in the current study indicate that Curcumin can suppress NF- $\kappa$ B and IKK activity; COX-2, PGE-2, and IL-8 expression; and cell proliferation in pancreatic malignancies, and all of these Curcumin-induced changes are associated with potent proapoptotic effects.

Some groups have [61] exploited an *in vitro* model of human tenocytes to study the mechanism of Curcumin on IL-1 $\beta$  signaling and investigate whether Curcumin might antagonize the catabolic effects of pro-inflammatory cytokines by suppressing NF- $\kappa$ B-activation and NF- $\kappa$ B induced gene expression. This study also explored the molecular mechanisms by which Curcumin suppresses NF- $\kappa$ B activation in tenocytes – a process that was partly mediated by the PI-3K/Akt signaling pathway. Overall, their data suggested that Curcumin down-regulates NF- $\kappa$ B and NF- $\kappa$ B- regulated gene products involved in apoptosis, matrix degradation and inflammation in human tenocytes *in vitro*.

It has also been shown that [62] turmeric can effectively block the proliferation of tumor cells through the suppression of NF- $\kappa$ B and STAT3 pathways.

It is worth to mention again that sometimes the general name of NF- $\kappa$ B and sometimes p65 is mentioned as a subunit of NF- $\kappa$ B in the works done above.

This study investigated the effects of co-administration of nano-Curcumin on anticancer effect of nano-Pirarubicin. We used Curcumin and Pirarubicin in different time intervals: before chemotherapy, after chemotherapy and at the same time, to show if there is any difference in the effect of Curcumin on viability of cancer cells in these three conditions.

In addition, we measured the differences of NF-κB levels in two different situations: when Pirarubicin is used alone and when it is mixed with Curcumin. The results of the study showed that there was no significant difference between the effects of Curcumin on viability of cancer cells in these three conditions: before chemotherapy, after chemotherapy and at the same time.

So it can be concluded that according to the results of this *in vitro* study, there is not any significant difference between administrating Curcumin to patient before or after Pirarubicin as a chemotherapy treatment. However, *in vivo* experiments can pave the way for a better understanding of the involved processes. It worth to mention that different natural products may show different co administration effect on the cytotoxicity and NF-κB level with different chemotherapy agents. For example, our research group previously found difference in different administrations of curcumin with paclitaxel [63]. The ratio of the amount of Curcumin to chemotherapy agent is also an important factor to be considered while investigating the effect of Curcumin in chemotherapy treatment.

Both C-SSM showed mono-dispersed size distribution consisted of 12.81 nm and DSC results revealed that Pirarubicin incorporates with SSM at both hydrophobic core and hydrophilic shell while Curcumin is more similarly to be settled at the hydrophobic core of SSM. All of these results indicate the suitability of these nano-formulations to be used as targeted cancer therapy agents.

Zhang et al [64] determined solubility of Curcumin to be 11 ng/mL at pH=5.5. Considering the fact that acidic media helps the solubility and by assuming solubility of Curcumin to be 6 ng/mL at neutral pH and room temperature, solubility of Curcumin is more than 33000 times enhanced in C-SSM formulation. We also showed that the stability of curcumin is enhanced in the lyophilized SSM formulation to be used in clinical applications. This is where the stability of free curcumin has been reported as not more than two hours [65]. These results are in well accordance with previously reported data [36, 37].

As it is explained at the results obtained from the NMR spectra, the majority of Curcumin structure is consisted of its enol tautomer, however, the β-diketo tautomer is still presented in the system. This hypothesis could explain the results obtained from DSC thermogram. Curcumin destroys SSM thermogram in all areas. This probably is due to its incorporation with both hydrophilic and hydrophobic parts of DSPE-PEG. This is where Pirarubicin is incorporated only with the hydrophobic part of SSM consisted of DSPE. This study also demonstrated the enhancement on the efficacy of Curcumin upon encapsulation inside of the nano-drug delivery system. Furthermore, we demonstrated successful inhibition of P65 using nano-curcumin, while this sub-unit of NF-κB was strongly increased by the chemotherapeutic agent Pirarubicin. Consequently, MDR was successfully inhibited using nano formulated curcumin.

## Acknowledgments

This work was partially supported by Bezmialem University Scientific Project Supporting Program No: 6.2018/10 and Research Fund of the Yildiz Technical University, Projects No: FDK-2017-3111. We would like to thank Prof. Dr. Mutlu Demiray for contributing in planning the study to test the hypothesis. We really appreciate the help of Dr. İlker Ün in recording the NMR data and Dr. Binnur Temel for the DSC data.

Supporting Information accompanies this paper on <http://www.acgpubs.org/journal/records-of-natural-products>

## ORCID

Zahra Eskandari: [0000-0003-4277-703X](#)

Fatemeh Bahadori: [0000-0003-4224-9309](#)

Melda Altikatoglu: [0000-0002-0800-1249](#)

Vildan Betul Yenigun: [0000-0002-8021-8629](#)

Abdurrahim Kocyigit: [0000-0003-2335-412X](#)

Hayat Onyuksel: [0000-0002-2693-4069](#)

## References

- [1] A. Shehzad, F. Wahid and Y.S. Lee (2010). Curcumin in cancer chemoprevention: Molecular targets, pharmacokinetics, bioavailability, and clinical trials, *Arch. Pharm. (Weinheim)*. **343**, 489-499.
- [2] S. Toden and A. Goel (2017). The holy grail of curcumin and its efficacy in various diseases: Is bioavailability truly a big concern?, *J. Restorat. Medic.* **6**, 27-36.
- [3] M. López-Lázaro (2008). Anticancer and carcinogenic properties of curcumin: Considerations for its clinical development as a cancer chemopreventive and chemotherapeutic agent, *Mol. Nutr. Food Res.* **52**, S103-S127.
- [4] D. Sinha, J. Biswas, B. Sung, B.B. Aggarwal and A. Bishayee (2012). Chemopreventive and chemotherapeutic potential of curcumin in breast cancer, *Curr. Drug Targets.* **13**, 1799-1819.
- [5] T. Esatbeyoglu, K. Ulbrich, C. Rehberg, S. Rohn and G. Rimbach (2015). Thermal stability, antioxidant, and anti-inflammatory activity of curcumin and its degradation product 4-vinyl guaiacol, *Food Funct.* **6**, 887-893.
- [6] K. Pan, H. Chen, S.J. Baek and Q. Zhong (2018). Self-assembled curcumin-soluble soybean polysaccharide nanoparticles: Physicochemical properties and in vitro anti-proliferation activity against cancer cells, *Food Chem.* **246**, 82-89.
- [7] A. Enomoto, K. Miyagawa and J. Yamada (2016). Mechanism of anticarcinogenic properties of curcumin and its application for radio-sensitization and clinical treatment, *Hoshas. Seibus. Kenkyu.* **51**, 115-126.
- [8] B.H. Choi, C.G. Kim, Y. Lim, S.Y. Shin and Y.H. Lee (2008). Curcumin down-regulates the multidrug-resistance mdr1b gene by inhibiting the pi3k/akt/nfkb pathway, *Cancer Lett.* **259**, 111-118.
- [9] B.B. Aggarwal (2004). Nuclear factor- $\kappa$ b: The enemy within, *Cancer Cell.* **6**, 203-208.
- [10] S. Shishodia, H.M. Amin, R. Lai and B.B. Aggarwal (2005). Curcumin (diferuloylmethane) inhibits constitutive nf- $\kappa$ pab activation, induces g1/s arrest, suppresses proliferation, and induces apoptosis in mantle cell lymphoma, *Biochem Pharmacol.* **70**, 700-713.
- [11] R.J. Anto, T.T. Maliekal and D. Karunagaran (2000). L-929 cells harboring ectopically expressed rela resist curcumin-induced apoptosis, *J. Biol. Chem.* 1-23, 10.1074/jbc.C000105200
- [12] G.R. Pillai, A.S. Srivastava, T.I. Hassanein, D.P. Chauhan and E. Carrier (2004). Induction of apoptosis in human lung cancer cells by curcumin, *Cancer Lett.* **208**, 163-170.
- [13] N.D. Perkins (2007). Integrating cell-signalling pathways with nf- $\kappa$ b and ikk function, *Nat. Rev. Mol. Cell. Biol.* **8**, 49-62.
- [14] S.D. Westerheide, M.W. Mayo, V. Anest, J.L. Hanson and A.S. Baldwin (2001). The putative oncoprotein bcl-3 induces cyclin d1 to stimulate g1 transition, *Mol. Cell. Biol.* **21**, 8428-8436.
- [15] D.W. Kim, L. Gazourian, S.A. Quadri, D.H. Sherr and G.E. Sonenshein (2000). The rela nf- $\kappa$ b subunit and the aryl hydrocarbon receptor (ahr) cooperate to transactivate the c-myc promoter in mammary cells, *Oncogene* **19**, 5498.
- [16] E.L. Lagow and D.D. Carson (2002). Synergistic stimulation of muc1 expression in normal breast epithelia and breast cancer cells by interferon- $\gamma$  and tumor necrosis factor- $\alpha$ , *J. Cell. Biochem.* **86**, 759-772.
- [17] L. Shen, C.-C. Liu, C.-Y. An and H.-F. Ji (2016). How does curcumin work with poor bioavailability? Clues from experimental and theoretical studies, *Sci. Rep.* **6**, 20872.
- [18] P. Anand, A.B. Kunnumakkara, R.A. Newman and B.B. Aggarwal (2007). Bioavailability of curcumin: Problems and promises, *Mol. Pharmaceutics.* **4**, 807-818.
- [19] A. Sarkar, R. De and A.K. Mukhopadhyay (2016). Curcumin as a potential therapeutic candidate for helicobacter pylori associated diseases, *World J. Gastroenterol.* **22**, 2736-2748.
- [20] F. Bahadori, A. Kocyigit, H. Onyuksel, A. Dag and G. Topcu (2017). Cytotoxic, apoptotic and genotoxic effects of lipid-based and polymeric nano micelles, an in vitro evaluation, *Toxics.* **6**, pii: E7. doi: 10.3390/toxics6010007.
- [21] H. Umezawa, Y. Takahashi, M. Kinoshita, H. Naganawa, T. Masuda, M. Ishizuka, K. Tatsuta and T. Takeuchi (1979). Tetrahydropyranyl derivatives of daunomycin and adriamycin, *The J. Antibiot.* **32**, 1082-1084.
- [22] A.A. Miller and E. Salewski (1994). Prospects for pirarubicin, *Med. Pediatr. Oncol.* **22**, 261-268.
- [23] T. Tsuruo, H. Iida, S. Tsukagoshi and Y. Sakurai (1981). Overcoming of vincristine resistance in p388 leukemia in vivo and in vitro through enhanced cytotoxicity of vincristine and vinblastine by verapamil, *Cancer Res.* **41**, 1967-1972.
- [24] S. Kunimoto, K. Miura, Y. Takahashi , T. Takeuch and H. Umezawa (1983). Rapid uptake by cultured tumor cells and intracellular behavior of 4'-o-tetrahydropyranyladriamycin, *The J. Antibiot.* **36**, 312-317.

- [25] P. Sadatmousavi and P.J.I.j.o.m.s. Chen (2013). Self/co-assembling peptide, ear8-ii, as a potential carrier for a hydrophobic anticancer drug pirarubicin (thp)—characterization and in-vitro delivery, **14**, 23315-23329.
- [26] R.L. Mancera, M. Chalaris and J. Samios (2004). The concentration effect on the ‘hydrophobic’ and ‘hydrophilic’ behaviour around dmso in dilute aqueous dmso solutions. A computer simulation study, *J. Mol. Liq.* **110**, 147-153.
- [27] F. Payton, P. Sandusky and W.L. Alworth (2007). Nmr study of the solution structure of curcumin, *J. Nat. Prod.* **70**, 143-146.
- [28] R. Benassi, E. Ferrari, S. Lazzari, F. Spagnolo and M. Saladini (2008). Theoretical study on curcumin: A comparison of calculated spectroscopic properties with nmr, uv-vis and ir experimental data, *J. Mol. Struct.* **892**, 168-176.
- [29] E. Gulcur, M. Thaqi, F. Khaja, A. Kuzmis and H. Onyuksel (2013). Curcumin in vip-targeted sterically stabilized phospholipid nanomicelles: A novel therapeutic approach for breast cancer and breast cancer stem cells, *Drug Deliv Transl Res.* **3** doi:10.1007/s13346-013-0167-6.
- [30] A. Banerjee and H. Onyuksel (2012). Human pancreatic polypeptide in a phospholipid-based micellar formulation, *Pharm. Res.* **29**, 1698-1711.
- [31] F. Bahadori, G. Topçu, M.S. Eroğlu and H. Önyüksel (2014). A new lipid-based nano formulation of vinorelbine, *AAPS Pharm. Sci. Tech.* **15**, 1138-1148.
- [32] S.B. Lim, I. Rubinstein and H. Onyuksel (2008). Freeze drying of peptide drugs self-associated with long-circulating, biocompatible and biodegradable sterically stabilized phospholipid nanomicelles, *Int. J. Pharm.* **356**, 345-350.
- [33] S.-i. Kawano, Y. Inohana, Y. Hashi and J.-M. Lin (2013). Analysis of keto-enol tautomers of curcumin by liquid chromatography/mass spectrometry, *Chin. Chem. Lett.* **24**, 685-687.
- [34] M. Reichenbächer and J. Popp, *Challenges in molecular structure determination*. 2012: Springer Berlin Heidelberg.
- [35] A.C. Gören, S. Çikrikçi, M. Çergel and G. Bilsel (2009). Rapid quantitation of curcumin in turmeric via nmr and lc–tandem mass spectrometry, *Food Chem.* **113**, 1239-1242.
- [36] E. Gültür, M. Thaqi, F. Khaja, A. Kuzmis and H. Önyüksel (2013). Curcumin in vip-targeted sterically stabilized phospholipid nanomicelles: A novel therapeutic approach for breast cancer and breast cancer stem cells, *Drug Del. Translat. Res.* **3**, 562-574.
- [37] E. Gulcur and H. Onyuksel, *A novel vasoactive intestinal peptide-grafted curcumin nanomedicine for targeting breast cancer stem cells*. 2012, AACR DOI: 10.1158/1538-7445.AM2012-1944.
- [38] K.W. Powers, M. Palazuelos, B.M. Moudgil and S.M. Roberts (2007). Characterization of the size, shape, and state of dispersion of nanoparticles for toxicological studies, *Nanotoxicology* **1**, 42-51.
- [39] M. Gera, N. Sharma, M. Ghosh, D.L. Huynh, S.J. Lee, T. Min, T. Kwon and D.K. Jeong (2017). Nanoformulations of curcumin: An emerging paradigm for improved remedial application, *Oncotarget* **8**, 66680 66698.
- [40] C. Foged, B. Brodin, S. Frokjaer and A. Sundblad (2005). Particle size and surface charge affect particle uptake by human dendritic cells in an in vitro model, *Int. J. Pharm.* **298**, 315-322.
- [41] G.a. He, H. Liu, R. Chen and C. Wang (2013). Transport behavior of engineered nanosized photocatalytic materials in water, *J. Nanomater.* **2013**, 3 Article ID 856387, 13 pages, <http://dx.doi.org/10.1155/2013/856387>.
- [42] F. Alexis, E. Pridgen, L.K. Molnar and O.C. Farokhzad (2008). Factors affecting the clearance and biodistribution of polymeric nanoparticles, *Mol. Pharm.* **5**, 505-515.
- [43] D. Deeb, X. Gao, A.S. Arbab, K. Barton, S.A. Dulchavsky and S.C. Gautam (2010). Cddo-me: A novel synthetic triterpenoid for the treatment of pancreatic cancer, *Cancers (Basel)* **2**, 1779-1793.
- [44] G. Yang, X. Xiao, D.G. Rosen, X. Cheng, X. Wu, B. Chang, G. Liu, F. Xue, I. Mercado-Uribe, P. Chiao, X. Du and J. Liu (2011). The biphasic role of nf-κb in progression and chemoresistance of ovarian cancer, *Clin. Cancer Res* **17**, 2181-2184.
- [45] A. Kawiak and A. Domachowska (2016). Plumbagin suppresses the invasion of her2-overexpressing breast cancer cells through inhibition of ikkalpha-mediated nf-kappab activation, *PLoS One* **11**, e0164064.
- [46] L. Vermeulen, G. De Wilde, S. Notebaert, W.V. Berghe and G. Haegeman (2002). Regulation of the transcriptional activity of the nuclear factor-κb p65 subunit, *Biochem. Pharmacol.* **64**, 963-970.
- [47] B.B. Aggarwal and B. Sung (2011). Nf-κb in cancer: A matter of life and death, *Cancer Discov.* **1**, 469-471.
- [48] M. Shakibaei, T. John, G. Schulze-Tanzil, I. Lehmann and A. Mobasher (2007). Suppression of nf-κb activation by curcumin leads to inhibition of expression of cyclo-oxygenase-2 and matrix metalloproteinase-9 in human articular chondrocytes: Implications for the treatment of osteoarthritis, *Biochem Pharmacol.* **73**, 1434-1445.

- [49] E.A. Comen, R.L. Bowman and M. Kleppe (2018). Underlying causes and therapeutic targeting of the inflammatory tumor microenvironment, *Front. Cell Dev. Biol.* **12**(6), 56. doi: 10.3389/fcell.2018.00056.
- [50] M.T. Harte, J.J. Gorski, K.I. Savage, J.W. Purcell, E.M. Barros, P.M. Burn, C. McFarlane, P.B. Mullan, R.D. Kennedy and N.D. Perkins (2014). Nf- $\kappa$ b is a critical mediator of brca1-induced chemoresistance, *Oncogene* **33**, 713-723.
- [51] P. Huang, D. Wang, Y. Su, W. Huang, Y. Zhou, D. Cui, X. Zhu and D. Yan (2014). Combination of small molecule prodrug and nanodrug delivery: Amphiphilic drug-drug conjugate for cancer therapy, *JACS*. **136**, 11748-11756.
- [52] P. Zou, J. Song, B. Jiang, F. Pei, B. Chen, X. Yang, G. Liu and Z. Hu (2014). Epigallocatechin-3-gallate protects against cisplatin nephrotoxicity by inhibiting the apoptosis in mouse, *Int. J. Clin. Exp. Pathol.* **7**, 4607-4616.
- [53] X. Duan, J. Xiao, Q. Yin, Z. Zhang, H. Yu, S. Mao and Y. Li (2013). Smart ph-sensitive and temporal-controlled polymeric micelles for effective combination therapy of doxorubicin and disulfiram, *ACS Nano* **7**, 5858-5869.
- [54] C.-Y. Wang, J.C. Cusack Jr, R. Liu and A.S. Baldwin Jr (1999). Control of inducible chemoresistance: Enhanced anti-tumor therapy through increased apoptosis by inhibition of nf- $\kappa$ b, *Nat. Med.* **5**, 412-417.
- [55] M. Kortylewski, R. Jove and H. Yu (2005). Targeting stat3 affects melanoma on multiple fronts, *Cancer Metastasis Rev.* **24**, 315-327.
- [56] M. Chaturvedi, B. Sung, V. Yadav, R. Kannappan and B. Aggarwal (2011). Nf- $\kappa$ b addiction and its role in cancer: 'One size does not fit all', *Oncogene* **30**, 1615-1630.
- [57] J.T. Sims, S.S. Ganguly, H. Bennett, J.W. Friend, J. Tepe and R. Plattner (2013). Imatinib reverses doxorubicin resistance by affecting activation of stat3-dependent nf- $\kappa$ b and hsp27/p38/akt pathways and by inhibiting abcb1, *PLoS One* **8**, e55509.
- [58] J.C. Cusack, R. Liu and A.S. Baldwin (1999). Nf-  $\kappa$ b and chemoresistance: Potentiation of cancer drugs via inhibition of nf-  $\kappa$ b, *Drug Resist. Upd.* **2**, 271-273.
- [59] M. Serasanambati, S.R. Chilakapati, P.K. Manikonda and J.R. Kanala (2013). Curcumin potentiates antitumor effect of gemcitabine in human breast cancer in vitro, *Curr. Trends Biotechnol. Pharm.* **7**, 854-861.
- [60] L. Li, B.B. Aggarwal, S. Shishodia, J. Abbruzzese and R. Kurzrock (2004). Nuclear factor- $\kappa$ b and ikb kinase are constitutively active in human pancreatic cells, and their down-regulation by curcumin (diferuloylmethane) is associated with the suppression of proliferation and the induction of apoptosis, *Cancer: Interdis. Int. J. Am. Cancer Soc.* **101**, 2351-2362.
- [61] C. Buhrmann, A. Mobasher, F. Busch, C. Aldinger, R. Stahlmann, A. Montaseri and M. Shakibaei (2011). Curcumin modulates nf- $\kappa$ b-mediated inflammation in human tenocytes in vitro: Role of the phosphatidylinositol 3-kinase-akt pathway, *J. Biol. Chem.* jbc. M111. 256180.
- [62] J.H. Kim, S.C. Gupta, B. Park, V.R. Yadav and B.B. Aggarwal (2012). Turmeric (*Curcuma longa*) inhibits inflammatory nuclear factor (nf)- $\kappa$ b and nf- $\kappa$ b-regulated gene products and induces death receptors leading to suppressed proliferation, induced chemosensitization, and suppressed osteoclastogenesis, *Mol. Nutr. Food Res.* **56**, 454-465.
- [63] F. Kazdal, F. Bahadori, Z. Eskandari, A. Kocyigit, B.O. Oztenekci and B. Çelik.(2018) In-vitro investigation of changes in efficacy and toxicity of nano-paclitaxel during co-applications with antioxidant natural compounds, in *24th World Nano Conference*.
- [64] H. Yu and Q. Huang (2010). Enhanced in vitro anti-cancer activity of curcumin encapsulated in hydrophobically modified starch, *Food Chem.* **119**, 669-674.
- [65] O. Naksuriya, M.J. van Steenbergen, J.S. Torano, S. Okonogi, and W.E. Hennink (2016). A kinetic degradation study of curcumin in its free form and loaded in polymeric micelles, *The AAPS J.* **18**, 777-787.